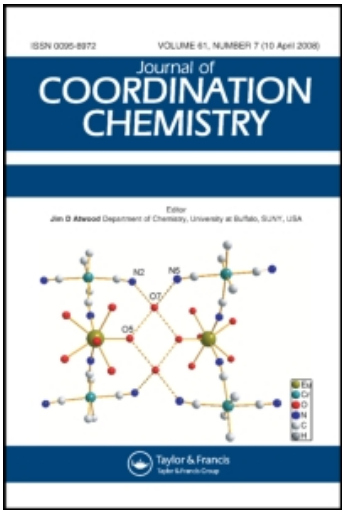

Journal of Coordination Chemistry
Publication details, including instructions for authors and subscription information:
http://www.informaworld.com/smpp/title~content=t713455674

Hydrothermal syntheses and crystal structures of hybrid materials based on Keggin cluster modified by iron complexes

Jingquan Sha[ab]; Jun Peng[a]; Hongsheng Liu[a]; Jing Chen[a]; Aixiang Tian[a]; Baoxia Dong[a]; Pengpeng Zhang[a]
[a] Faculty of Chemistry, Key Laboratory of Polyoxometalate Science of Ministry of Education, Northeast Normal University, Changchun, Jilin 130024, P.R. China [b] Faculty of Chemistry and Pharmacy, Jiamusi University, Jiamusi, Heilong, Jiang 154007, P.R. China

First published on: 19 September 2007

To cite this Article Sha, Jingquan , Peng, Jun , Liu, Hongsheng , Chen, Jing , Tian, Aixiang , Dong, Baoxia and Zhang, Pengpeng(2008) 'Hydrothermal syntheses and crystal structures of hybrid materials based on Keggin cluster modified by iron complexes', Journal of Coordination Chemistry, 61: 8, 1221 — 1233, First published on: 19 September 2007 (iFirst)
To link to this Article: DOI: 10.1080/00958970701515658
URL: http://dx.doi.org/10.1080/00958970701515658

Journal of Coordination Chemistry
Vol. 61, No. 8, 20 April 2008, 1221–1233

Hydrothermal syntheses and crystal structures of hybrid materials based on Keggin cluster modified by iron complexes

JINGQUAN SHA†‡, JUN PENG*†, HONGSHENG LIU†, JING CHEN†, AIXIANG TIAN†, BAOXIA DONG† and PENGPENG ZHANG†

†Faculty of Chemistry, Key Laboratory of Polyoxometalate Science of Ministry of Education, Northeast Normal University, Changchun, Jilin 130024, P.R. China
‡Faculty of Chemistry and Pharmacy, Jiamusi University, Jiamusi, Heilong, Jiang 154007, P.R. China

(*Received 29 June 2007; in final form 4 July 2007*)

Three new organic-inorganic hybrid complexes based on the Keggin polyoxometalates (POMs) modified by transition metal iron and *N*-ligand organic moiety: $[Fe(phen)_3]_2[PMo_7^{VI}Mo_5^{V}O_{40}V^{IV}O]$ (**1**) $[Fe(phen)_2(H_2O)]_2[PMo_{11}^{VI}Mo^{V}O_{40}]\cdot 2H_2O$ (**2**) and $[Fe(phen)_3]_2[GeMo_{10}^{VI}Mo_2^{V}O_{40}]\cdot 0.5H_2O$ (**3**) (phen = 1,10-phenanthroline) have been hydrothermally synthesized and structurally characterized. Crystal data for complex **1**: $C_{72}H_{48}Fe_2M_{12}N_{12}O_{41}PV$, triclinic, $P\bar{1}$, $a = 11.6618(2)$ Å, $b = 13.8523(2)$ Å, $c = 14.9168(2)$ Å, $\alpha = 105.87(3)^\circ$, $\beta = 93.103(2)^\circ$, $\gamma = 96.609(2)^\circ$, $V = 2293.2(5)$ Å^3, $Z = 1$; for complex **2**: $C_{48}H_{32}Fe_2PMo_{12}N_8O_{44}$, triclinic, $P\bar{1}$, $a = 10.961(2)$ Å, $b = 13.357(3)$ Å, $c = 13.701(3)$ Å, $\alpha = 69.09(3)^\circ$, $\beta = 71.37(3)^\circ$, $\gamma = 78.21(3)^\circ$, $V = 1766.4(6)$ Å^3, $Z = 1$; for complex **3**: $C_{72}H_{50}Fe_2Mo_{12}N_{12}O_{41}Ge$, triclinic, $P\bar{1}$, $a = 12.160(2)$ Å, $b = 13.676(3)$ Å, $c = 14.627(3)$ Å, $\alpha = 105.05(3)^\circ$, $\beta = 109.64(3)^\circ$, $\gamma = 93.07(3)^\circ$, $V = 2185.6(7)$ Å^3, $Z = 1$. Other characterizations by element analysis, IR, XPS and TGA analysis are also described. Their electrochemical properties have been studied in the paper.

Keywords: Keggin structure; Polyoxometalates; Iron; Hydrothermal synthesis; Electrochemical property

1. Introduction

Inorganic–organic hybrid materials have potential applications in fields such as medicine, catalysis, ion exchange, molecular materials, photochemical, electrochemistry and magnetism [1, 2]. Design and synthesis of novel inorganic–organic solid materials based on modified Keggin polyoxometalates (POMs) and their derivatives is a challenge. Decoration of polyoxoanions with transition metal complexes of various organic groups provides a powerful method for their functionalization and immobilization combining the features and properties of both subunits and enriching

*Corresponding author. Email: jpeng@nenu.edu.cn

ISSN 0095-8972 print/ISSN 1029-0389 online © 2008 Taylor & Francis
DOI: 10.1080/00958970701515658

the chemistry of POM-based hybrids [3]. Some successful examples of heteropolyanion cluster-supported transition metal complexes include $[\{Cu_4(terpy)_4(PO_4)(H_2O)_2\}\{W_{10}(VI)W_2(V)O_{36}(PO_4)\}]\cdot 5H_2O$ [4], $[Ni(2,2'\text{-bipy})_3]_{1.5}[PW_{12}O_{40}Ni(2,2'\text{-bipy})_2(H_2O)]\cdot 0.5H_2O$ [5], $[PW_9V_3O_{40}\{Ag(2,2'\text{-bipy})\}_2\{Ag_2(2,2'\text{-bipy})_3\}_2]$ [6], and $2\text{-}2'\text{-bipy})_3]_2[ZnW_{12}O_{40}Zn(2\text{-}2'\text{-bipy})_2]\cdot H_2O$ [7]. Additionally, a number of capped pseudo-Keggin structures have been reported by Liu, Xu and our group [8]. In these structures, the transition metal coordination complexes provide charge compensation and also become a part of the inorganic POM framework. Although a large number of 3d transition metal complex-modified Keggin POM hybrids have been reported, Keggin POM-supported iron complexes are few [9]. Our group focused on modification of POMs, allowing synthesis of saturated Keggin POM modified by iron complex under hydrothermal conditions to obtain extended structures of new materials. Herein we report three novel complexes $[Fe(phen)_3]_2[PMo_7^{VI}Mo_5^{V}O_{40}V^{IV}O]$ (**1**), $[Fe(phen)_2(H_2O)]_2[PMo_{11}^{VI}Mo^{V}O_{40}]\cdot 2H_2O$ (**2**), and $[Fe(phen)_3]_2[GeMo_{10}^{VI}Mo_2^{V}O_{40}]\cdot 0.5H_2O$ (**3**). Complexes **1** and **3** consist of discrete polyoxoanion and counter chiral cation $[Fe(phen)_3]^{3+}$. In complex **2**, both $[Fe(phen)_2(H_2O)]^{2+}$ groups are coordinated to the α-Keggin-type polyoxoanion $[PMo_{11}^{VI}Mo^{V}O_{40}]^{6-}$ *via* the surface terminal oxygen atoms of two opposite oxygen atoms at the same equator surface.

2. Experimental

2.1. *General procedures*

All reagents were purchased commercially and used without further purification. All syntheses were carried out in 18 mL Teflon-lined autoclaves under autogenous pressure. Distilled water was used in the reactions. Elemental analyses (C, H, and N) were performed on a Perkin–Elmer 2400 CHN Elemental Analyzer. Fe and V were determined by a Leaman inductively coupled plasma (ICP) spectrometer. XPS analysis was performed on a VGESCALABMKII spectrometer with an Mg-Kα (1253.6 eV) achromatic X-ray source. The vacuum inside the analysis chamber was maintained at 6.2×10^{-6} Pa during analysis. The IR spectrum was obtained on an Alpha Centaurt FT/IR spectrometer with KBr pellets in the 400–4000 cm^{-1} region. TG analysis was performed on a DTG-60AH instrument in flowing N_2 with a heating rate of $10^{\circ}C\,min^{-1}$. Cyclic voltammograms were obtained with a CHI 660 electrochemical workstation at room temperature. Platinum gauze was used as counter electrode and Ag/AgCl electrode was reference. A chemically bulk-modified carbon paste electrode (CPE) was used as working electrode.

2.2. *Hydrothermal synthesis*

Synthesis of $[Fe(phen)_3]_2[PMo_7^{VI}Mo_5^{V}O_{40}V^{IV}O]$ (**1**). The starting materials $H_3[PMo_{12}O_{40}]\cdot XH_2O$, phen, Fe_2O_3, NH_4VO_3, trea (triethylamine) and distilled water in a molar ratio of ca 1 : 3 : 1 : 2 : 2 : 1000 were mixed. The resulting suspension was stirred for 1h and the pH was adjusted to 5.0 by 2 mol L^{-1} HCl. The mixture was then transferred into a Teflon-lined autoclave (18 mL) with 60% filling. After heating at 175°C for 5 days, the reactor was slowly cooled to room temperature. Black block

crystals of **1** were filtered, washed with water, and dried at room temperature (35% yield based on Fe). Anal. Calcd: C, 28.03; H, 1.56; N, 5.45; Fe, 3.63; V, 1.66. Found: C, 27.94; H, 1.49; N, 5.39; Fe, 3.68; V, 1.58(%).

Synthesis of $[Fe(phen)_2(H_2O)]_2[PMo^{VI}_{11}Mo^{V}O_{40}]\cdot 2H_2O$ (**2**). The synthetic method was similar to that used for the preparation of **1** except that the starting materials $H_3[PMo_{12}O_{40}]\cdot XH_2O$, phen, Fe_2O_3, NH_4VO_3, trea (triethylamine) and distilled water in a molar ratio of ca 1 : 3 : 1 : 1 : 2 : 1000 were replaced by 1 : 1.5 : 1 : 0.5 : 2 : 1000. Red-black block crystals of **2** were filtered, washed with water, and dried at room temperature (25% yield based on Fe). Anal. Calcd: C, 21.19; H, 1.17; N, 4.12; Fe, 4.12. Found: C, 21.80; H, 1.79; N, 4.01; Fe, 4.08 (%).

Synthesis of $[Fe(phen)_3]_2[GeMo^{VI}_{10}Mo^{V}_2O_{40}].0.5H_2O$ (**3**). The synthetic method is the same as **1**, with $H_4[GeMo_{12}O_{40}]\cdot XH_2O$[10], phen, Fe_2O_3, NH_4VO_3, trea and distilled water in a molar ratio of ca 1 : 3 : 1 : 0.5 : 2 : 1000 being mixed. Red block crystals of complex **3** were isolated, washed with distilled water and air-dried (30% yield based on Fe). Anal. Calcd: C, 28.12; H, 1.63; N, 5.47; Fe, 3.64; (%). Found: C, 28.44; H, 1.31; N, 5.23; Fe, 3.25.

2.3. *Structure determination*

Crystal data for complexes **1–3** were collected on a Rigaku RAXIS RAPID IP with Mo-Kα monochromatic radiation ($\lambda = 0.71073$ Å) at 293 K. The structures were solved by direct methods and refined by full matrix least-squares on F^2 using the SHELXTL crystallographic software package [11]. All non-hydrogen atoms were refined anisotropically. The positions of hydrogen atoms on carbon atoms were calculated theoretically. Crystallographic data are given in table 1. Selected bond distances and bond angles are given in table 2.

2.4. *Preparation of 1-, 2-, 3-CPE*

Complexes **1**, **2**, and **3** modified carbon paste electrode **1**-, **2**-, **3**-CPE were prepared as follows: 48 mg of graphite powder and 8 mg of complexes **1**, **2**, and **3** were mixed and ground together by agate mortar and pestle to achieve a uniform mixture, and then added to 0.6 mL nujol with stirring. The homogenized mixture was packed into a glass tube with 1.2 mm inner diameter, and the tube surface was wiped with paper. Electrical contact was established with copper rod through the back of the electrode.

3. Results and discussion

3.1. *Syntheses*

In the hydrothermal environment, the viscosity of the solvent results in enhanced rates of solvent extraction of solids and crystal growth from solution. Furthermore, since the problem of different solubilities is minimized, a variety of simple organic and/or inorganic template agents can be introduced. Therefore, the introduction of hydrothermal technique and direct use of saturated Keggin POM as building block

Table 1. Crystal data and structure refinement for **1**–**3**.

	1	**2**	**3**
Empirical formula	$C_{72}H_{48}Fe_2Mo_{12}N_{12}O_{41}PV$	$C_{48}H_{40}Fe_2Mo_{12}N_8O_{44}P$	$C_{72}H_{50}Fe_2Mo_{12}N_{12}O_{40.5}Ge$
CCDC	628082	619071	619083
Formula weight	3082.12	2726.77	3066.8
T (K)	293(2)	293(2)	293(2)
Wavelength (Å)	0.71073	0.71073	0.71073
Crystal system	Triclinic	Triclinic	Triclinic
Space group	$P\bar{1}$	$P\bar{1}$	$P\bar{1}$
a (Å)	11.662(2)	10.961(2)	12.160(2)
b (Å)	13.852(2)	13.357(3)	13.676(3)
c (Å)	14.917(2)	13.701(3)	14.627(3)
α (°)	105.871(2)	69.09(3)	105.05(3)
β (°)	93.103(2)	71.37(3)	109.64(3)
γ (°)	96.609(2)	78.21(3)	93.07(3)
V (Å^3)	2293.2(5)	1766.4(6)	2185.6(7)
Z	1	1	1
D_{Calcd} (mg m^{-3})	3.407	2.631	2.329
Absorption coefficient(mm^{-1})	6.794	2.588	2.414
F(000)	2176	1399	1476
Goodness-of-fit on F^2	1.037	1.071	1.032
Final R_1[a], wR_2[b] [$I>2\sigma(I)$]	$R_1=0.0652$, $wR_2=0.2059$	$R_1=0.0789$, $wR_2=0.2183$	$R_1=0.0643$, $wR_2=0.1796$
R indices (all data)	$R_1=0.1187$, $wR_2=0.2306$	$R_1=0.0925$, $wR_2=0.2330$	$R_1=0.0904$, $wR_2=0.1970$

[a] $R_1=\sum\|F_o|-|F_c\|/\sum|F_o|$. [b] $wR_2=\{\sum[w(F_o^2-F_c^2)^2]/\sum[w(F_o^2)^2]\}^{1/2}$.

Table 2. Selected bond lengths [A°] and angles [°] for **1–3**.

Complex **1**			
P(1)–O(2)#1	1.427(11)	V(1)–O(3)	1.670(15)
P(1)–O(7)	1.508(12)	V(1)–O(9)	1.906(9)
P(1)–O(1)	1.530(13)	V(1)–O(20)	1.902(8)
P(1)–O(4)#1	1.582(13)	V(1)–O(22)#1	2.064(9)
Fe(1)–N(5)	1.971(8)	V(1)–O(12)#1	2.074(10)
Fe(1)–N(6)	1.964(9)	Mo(1)–O(9)	1.954(8)
Fe(1)–N(1)	1.977(8)	Mo(1)–O(20)	1.952(7)
Fe(1)–N(3)	1.997(9)	Mo(1)–O(1)	2.465(13)
Fe(1)–N(4)	1.995(8)	Mo(1)–O(7)	2.501(13)
Fe(1)–N(2)	2.012(7)	Mo(1)–O(14)	1.859(9)
O(2)#1–P(1)–O(7)	65.8(6)	O(3)–V(1)–O(12)#1	118.0(6)
O(2)#1–P(1)–O(7)#1	114.2(6)	O(9)–V(1)–O(12)#1	130.4(5)
O(1)–P(1)–O(4)#1	77.0(6)	O(20)–V(1)–O(12)#1	79.1(3)
O(7)–P(1)–O(1)	71.1(6)	O(22)#1–V(1)–O(12)#1	76.7(3)
O(2)#1–P(1)–O(1)#1	65.9(7)	O(13)–Mo(1)–O(8)	101.4(5)
O(7)–P(1)–O(1)#1	108.9(6)	O(13)–Mo(1)–O(14)	101.7(5)
O(1)#1–P(1)–O(4)#1	103.0(6)	O(8)–Mo(1)–O(14)	90.4(4)
O(2)–P(1)–O(4)#1	108.5(6)	O(13)–Mo(1)–O(9)	101.9(4)
O(7)–P(1)–O(4)#1	107.3(6)	O(8)–Mo(1)–O(9)	88.6(4)
O(7)#1–P(1)–O(4)#1	72.7(6)	O(14)–Mo(1)–O(9)	156.1(5)
O(14)–Mo(1)–O(20)	89.4(3)	O(13)–Mo(1)–O(1)	158.4(4)
O(9)–Mo(1)–O(20)	82.3(3)	O(8)–Mo(1)–O(20)	156.7(4)
Complex **2**			
P(1)–O(24)#1	1.84(4)	Mo(1)–O(6)	1.632(16)
P(1)–O(19)	1.59(3)	Mo(1)–O(17)#1	1.890(16)
P(1)–O(9)	1.72(3)	Mo(1)–O(11)	1.890(19)
P(1)–O(20)	1.69(3)	Mo(1)–O(7)	1.892(16)
O(1)–Fe(1)	2.187(1)	Mo(1)–O(18)	1.959(16)
N(1)–Fe(1)	2.128(18)	Mo(1)–O(19)	2.35(3)
Fe(1)–N(2)	2.033(18)	Mo(1)–O(20)#1	2.46(3)
Fe(1)–N(3)	2.092(18)	O(17)–Mo(1)#1	1.890(16)
Fe(1)–OW2	2.144(16)	Fe(1)–N(4)	2.146(16)
Complex **3**			
Ge(1)–O(9)#1	1.787(10)	Fe–N(1)	1.970(7)
Ge(1)–O(24)#1	1.653(11)	Fe–N(5)	1.975(7)
Ge(1)–O(8)#1	1.675(11)	Fe–N(3)	1.976(7)
Ge(1)–O(19)#1	1.779(10)	Fe–N(2)	1.984(7)
Mo(1)–O(24)#1	2.434(10)	Fe–N(6)	1.984(7)
Mo(1)–O(4)	1.645(7)	Fe–N(4)	1.996(7)
Mo(1)–O(22)	1.857(9)	Mo(1)–O(16)#1	1.934(8)
Mo(1)–O(2)	1.895(8)	Mo(1)–O(9)	2.292(10)
Mo(1)–O(13)	1.904(9)	O(24)–Mo(1)#1	2.434(10)

Symmetry transformations used to generate equivalent atoms: $\#1 - x, -y, -z+1$ for **1**; $\#1 - x+3, -y-2, -z-1$ for **2**; $\#1 - x+1, -y+1, -z+1$ for **3**.

may produce a large number of novel organic-inorganic hybrid materials. In principle, the hydrothermal synthesis has many variables such as initial reactants and their stoichiometry, pH, crystallization temperature and pressure, which can affect the result significantly [12]. During our research, we observed that the coordination competition of complexes **1**–**3** depends on the stoichiometry in the self-assembly process under hydrothermal conditions. Additionally, in the synthesis reactions, it seemed as if NH_4VO_3 would not play any part in assembly of complexes **2** and **3**, but we tried to synthesize **2** and **3** under the same conditions without NH_4VO_3, no crystal was observed.

3.2. *Description of the structures*

3.2.1. $[Fe(phen)_3]_2[PMo_7^{VI}Mo_5^{V}O_{40}V^{IV}O]$ (1). Single crystal X-ray diffraction analysis reveals that **1** consists of discrete polyoxoanions $[PMo_7^{VI}Mo_5^{V}O_{40}V^{IV}O]^{6-}$ and counter cations $[Fe(phen)_3]^{3+}$ (see figure 1). Selected bond lengths and angles are collected in table 2. The polyoxoanion can be best described as one α-Keggin core$\{PMo_{12}O_{40}\}$ with $\{VO\}$ units capping two opposite pits which the V atoms half-occupied. Caps are formed through ligation of oxygen atoms on the two opposite $\{Mo_4O_4\}$ faces or pits to each $\{VO\}$ unit such that square pyramidal vanadium coordination environments are generated. The V–O bond lengths range from 1.670(15) to 2.074(2) Å, while the O–V–O angles are in the range 76.7(3)–130.4(5)°. All molybdenum atoms have a distorted $\{MoO_6\}$ octahedral environment with Mo–O distances in the range 1.617(8)–2.501(13) Å, and bond angles 62.4(4)–159.9(4)°. The disordered PO_4 tetrahedron, namely, the central atom P is surrounded by a cube of eight oxygen atoms, with each oxygen site half-occupied, was located in the center of the host cage with P–O average distance 1.512(2) Å and O–P–O bond angle in the range of 103.0(6)–114.2(6)°. The assignment of oxidation states for vanadium and molybdenum atoms is consistent with their coordination geometries and is confirmed by valence sum calculations [13], which gives the value for V is 3.96, with average value of Mo of 5.62. The calculated results reveal that in the polyoxoanion of **1**, the V center are in +4 oxidation state, while five out of twelve Mo centers are in the +5 oxidation state.

In the structure of **1**, there exists chiral complex cation $[Fe(phen)_3]^{3+}$. Each Fe atom is coordinated by six nitrogen atoms from three phen ligands to form a distorted FeN_6 octahedron with an isolated complex cation in the L/D configuration. The average Fe–N distance is 1.986 Å.

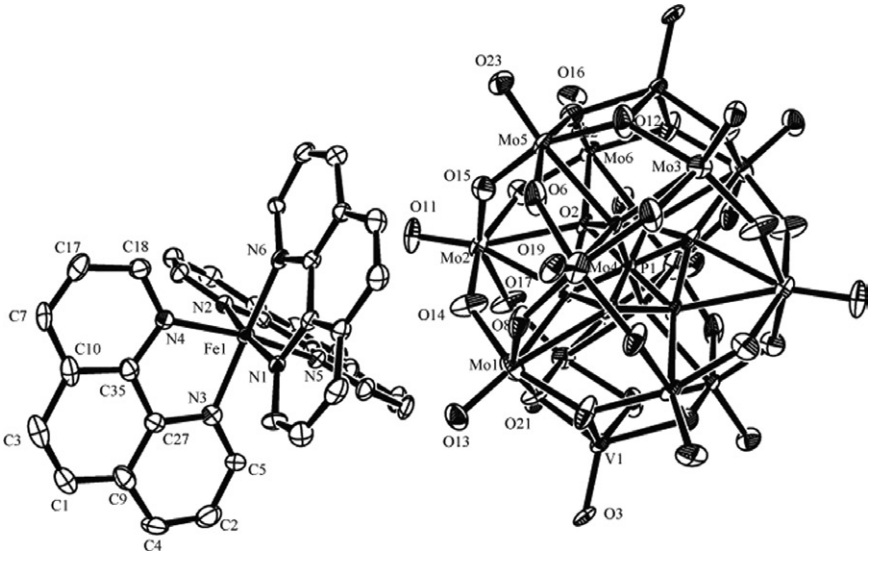

Figure 1. ORTEP drawing of **1** showing labeling of atoms with thermal ellipsoids at 30% probability level. (water molecules and H atoms are omitted for clarity).

3.2.2. $[Fe(phen)_2(H_2O)]_2[PMo_{11}^{VI}Mo^{V}O_{40}] \cdot 2H_2O$ (2). The single crystal structure analysis reveals that **2** is a neutral bisupporting complex based on the Keggin POM modified by iron complex: $[Fe(phen)_2(H_2O)]_2[PMo_{11}^{VI}Mo^{V}O_{40}].2H_2O$. As shown in figure 2, **2** is composed of a Keggin $[PMo_{11}^{VI}Mo^{V}O_{40}]^{4-}$ unit, two $[Fe(phen)_2(H_2O)]^{2+}$ fragments and two H_2O. For the polyoxoanion, the central atom P is located at the inversion center, which results in a disordered PO_4 tetrahedron, namely, the central atom P is surrounded by a cube of eight oxygen atoms, with each oxygen site half-occupied. Selected bond lengths are collected in table 2. The $[PMo_{11}^{VI}Mo^{V}O_{40}]^{4-}$ cluster possesses the classical α-Keggin type structure [14], similar to **1**. According to elemental analysis, bond valence sum (BVS) calculations, coordination geometries and charge balance, **2** is formulated as $[Fe(phen)_2(H_2O)]_2[PMo_{11}^{VI}Mo^{V}O_{40}] \cdot 2H_2O$. Using an empirical formula of bond valence, $S = \exp[\Sigma - (R - Ro)/B]$ ($S =$ bond valence, $R =$ bond length), the iron atoms are in the +2 oxidation state, while one molybdenum atom in the +5 oxidation state and the other molybdenum atoms are in the +6 oxidation state (the average calculated value is 5.96, compared to expected value of 5.92), confirming the molecular formula of **2**. The BVS values of the Mo atoms, however, do not clearly identify the reduced Mo site. This is due to possible delocalization of the d electrons of the reduced molybdenum centers over the polyanion framework involving all Mo's as observed in heteropolyblues.

The polyoxoanion acts as a ligand covalently bonding to two $[Fe(phen)_2(H_2O)]$ fragments through its terminal oxygen atoms with Fe–O(1) distances of 2.186(6) Å. The Fe atom is coordinated by one terminal oxygen atom O(1) of the Keggin anion, four nitrogen atoms from two phen ligands with Fe–N distances of 2.032(7)–2.140(3) Å and an aqua ligand, forming a distorted octahedron.

3.2.3. $[Fe(phen)_3]_2[GeMo_{10}^{VI}Mo_2^{V}O_{40}] \cdot 0.5H_2O$ (3). Complex **3** consists of discrete polyoxoanions $[GeMo_{10}^{VI}Mo_2^{V}O_{40}]^{6-}$, counter cations $[Fe(phen)_3]^{3+}$, and water molecules (figure 3). Selected bond lengths are collected in table 2. Similar to the complex **1**, the polyoxoanions $[GeMo_{10}^{VI}Mo_2^{V}O_{40}]^{6-}$ of **3** are α-Keggin core. All molybdenum atoms have a distorted $\{MoO_6\}$ octahedral environment with Mo–O distances in the range of 1.645(7)–2.434(10) Å. The disordered GeO_4 tetrahedron was located in the center of the

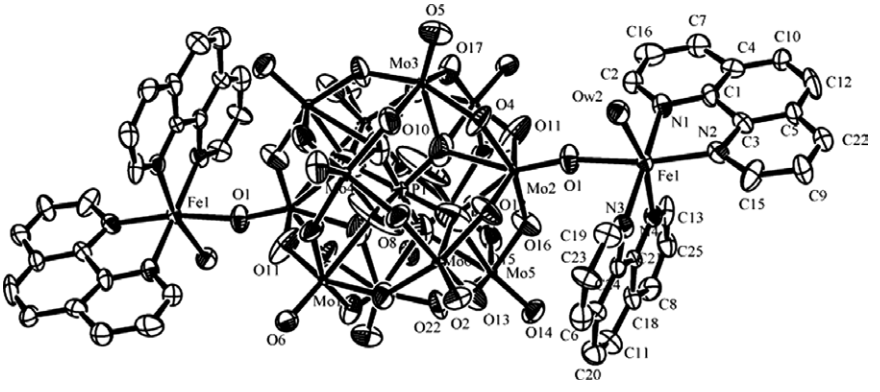

Figure 2. ORTEP drawing of **2** showing labeling of atoms with thermal ellipsoids at 40% probability level. (water molecules and H atoms are omitted for clarity).

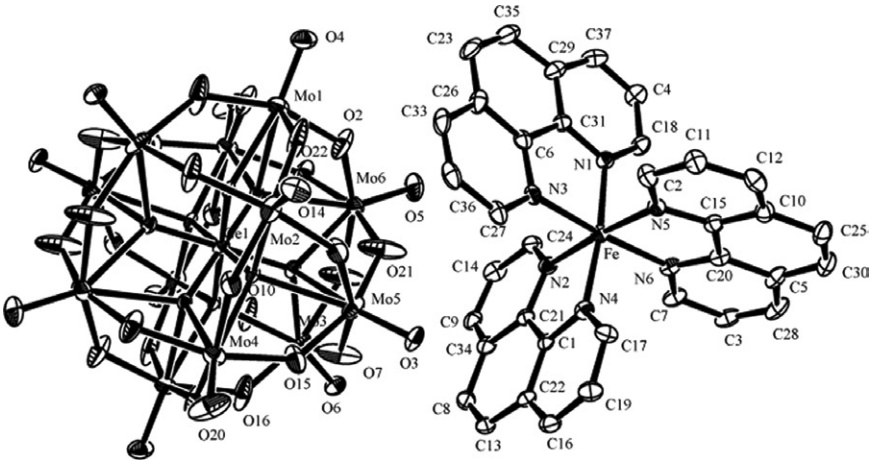

Figure 3. ORTEP drawing of **3** showing labeling of atoms with thermal ellipsoids at 30% probability level. (Water molecules and H atoms are omitted for clarity.)

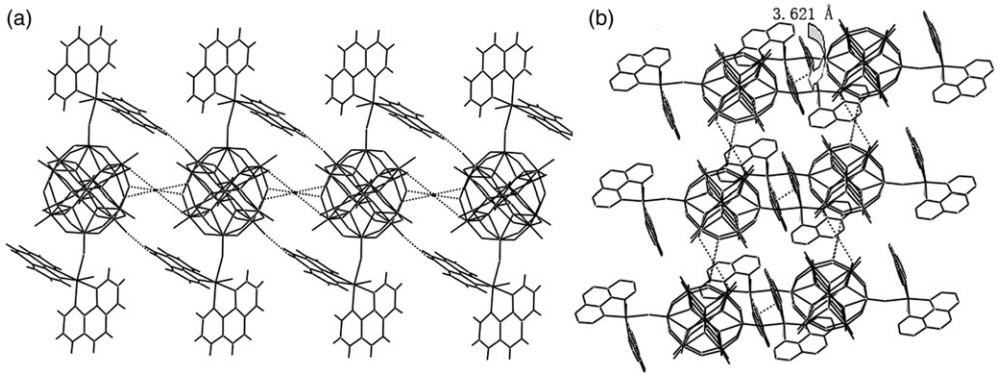

Figure 4. (a) View of 1D supramolecular chain with hydrogen bonding contacts along the α-axis in **2**; (b) $\pi\cdots\pi$ interactions in the 2D layer. Bonds are represented by broken lines.

host cage with Ge–O average distance 1.724(5) Å. The valence sum calculations show that two Mo atoms are in the +5 oxidation state and the iron atoms are in the +3 oxidation state, which are consistent with their coordination geometries, elemental analysis and charge balance. In the structure of **3**, there also exists chiral complex cation $[Fe(phen)_3]^{3+}$ which is the same as complex **1** and the average Fe–N distance is 1.981 Å.

Supramolecular interactions occur in the crystal structure of **2** and **3**. In **2**, these bisupporting Keggin anions are not discrete but linked to each other via water which caps over the surface window of a polyanion, giving rise to an infinite 1D chain along the *a*-axis as shown in figure 4(a). The distances of typical hydrogen bonds are Ow(3)···O(13) 2.697 Å, Ow(3)···O(18) 3.011 Å, Ow(3)···O(22) 2.870 Å. Hydrogen bonds and $\pi\cdots\pi$ stacking interactions (the shortest distance 2.621 Å) extend the 1D chains into 2D layers (figure 4b). These layers are further connected by short contacts into 3D a supermolecular framework.

In **3**, water molecules link adjacent polyoxoanions $[GeMo^{VI}_{10}Mo^{V}_{2}O_{40}]^{6-}$ and $[Fe(phen)_3]^{3+}$ together through hydrogen bonding interactions although the

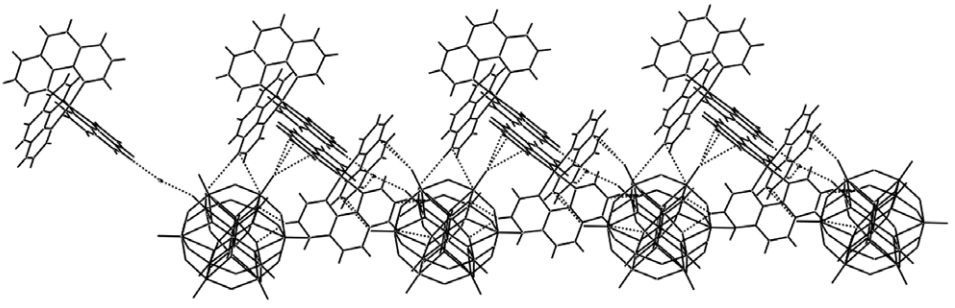

Figure 5. View of 1D supramolecular chain with hydrogen bonding contacts in **3**.

polyoxoanions are discrete from the view point of the covalent bond. Typical hydrogen bonds are Ow(5)···O(6) 2.700 Å and Ow(5)···H(30)C(30) 2.485 Å. Thus a 1D supramolecular chain is formed via hydrogen bonding interactions (see figure 5). Meanwhile, the neighboring anions and $[Fe(phen)_3]^{3+}$ are further connected via molecular interactions with the shortest C(24)···O(5) distance of 3.161(6) Å and C(14)···O(5) distance of 3.021(6) Å into the 3D supramolecular network.

3.3. *IR spectra, XPS spectra, TG analysis*

IR spectra of **1**–**3** exhibit similar absorption bands (see figure S1). The strong bands at 1054, 950, 878, 807 for **1**, 1056, 950, 887 and 802 cm^{-1} for **2** are ascribed to ν_{as}(P–O) ν_{as}(Mo–Od), ν_{as}(Mo–Ob–Mo) and ν_{as}(Mo–Oc–Mo) vibrations, and 790, 952, 894 and 718 cm^{-1} are attributed to ν_{as}(Ge–O), ν_{as}(Mo–Od), ν_{as}(Mo–Ob–Mo) and ν_{as}(Mo–Oc–Mo) vibrations for **2** (where O_d = terminal oxygen, O_c = bridged oxygen of two octahedrous sharing an edge), respectively [15], and characteristic bands of phen are in the 1420–1627 cm^{-1}. The XPS spectrum of **2** (figure S2) gives two overlapped peaks at 232.16 and 230.98 eV attributed to Mo^{6+} and Mo^{5+}. All these results further confirm the structure.

The TG curves of **1**–**3** (see figure S3) exhibit continuous weight loss in the temperature range of 20–600°C, ascribed to release of H_2O and phen molecules, and decomposition of POMs, respectively. For **2**, the first and second weight loss of 2.54% at 20–203°C correspond to loss of water, agreeing well with the calculated value of 2.35% for four H_2O per empirical formula unit. A noteworthy finding is that there is still weight loss above 600°C, indicating that these complexes are still being lost even at the upper limit of measurement range.

3.4. *Cyclic voltammetry*

To study redox properties of **1**–**3**, we used them as modifiers to fabricate chemically modified CPE owing to their insolubility in water and most organic solvents. The cyclic voltammetry (CV) of **1**-CPE, **2**-CPE and **3**-CPE were measured in the potential range from +1200 to −300 mV. In the potential range, we explored the typical cyclic

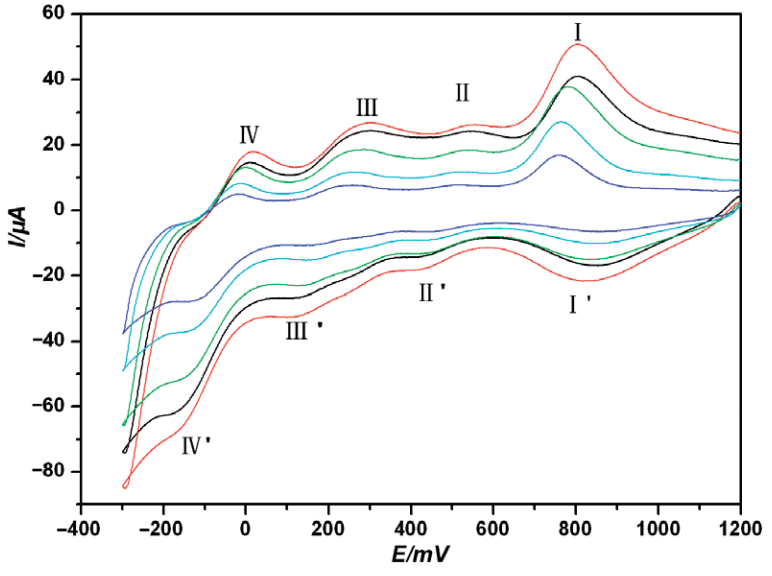

Figure 6. The cyclic voltammograms for **1**-CPE in $H_2SO_4 + Na_2SO_4$ aqueous solution at different scan rate (from inner to outer: 50, 100, 150, 200, 250 mV s^{-1}).

voltammetric behavior of them in $Na_2SO_4 + H_2SO_4$ aqueous solution (pH = 0.95) at different scan rates.

3.4.1. Voltammetric behaviors of 1-CPE and 2-CPE in aqueous. Figure 6 presents the voltammetric behavior for **1**-CPE at different scan rates. In the potential range from +1200 to −300 mV, four reversible redox peaks appeared and the mean peak potentials $E_{1/2} = (Epc + Epa)/2$ are 817.5, 483.5, 214 and −82 mV, respectively. Redox peaks I–I′ should be ascribed to the one-electron redox process of Fe (III/II). Redox peaks II–II′, III–III′, IV–IV′ corresponded to three consecutive two-electron processes of Mo, respectively. With the variation of scan rate from 50 to 200 mV s^{-1}, the cathodic peak currents were almost the same as the corresponding anodic ones [16], and the peak potentials of I–I′, II–II′, III–III′, IV–IV′ change gradually: the cathodic peak potentials shift toward the negative and the corresponding anodic peak potentials to the positive direction. The peak-to-peak separation between the corresponding cathodic and anodic peaks increases with increasing scan rate, but the mean peak potentials do not change on the whole. Figure 7 shows the voltammetric behavior for **2**-CPE at different scan rates. Similarly to the **1**-CPE, there exist four pairs of reversible redox peaks and the mean peak potentials $E_{1/2}$ are 820, 502, 236 and −48 mV, respectively. The values of $E_{1/2}$ in **2**-CPE shift to the positive direction as compared with **1**-CPE. The small difference in $E_{1/2}$ in **1** and **2** suggests the corresponding complex fragments have little influence on electrochemical behavior of **1**-CPE and **2**-CPE.

3.4.2. Voltammetric behavior of 3-CPE in aqueous. Figure 8 presents the voltammetric behavior for **3**-CPE at different scan rates. It can be clearly seen that in the potential range −300 to +1200 mV, four reversible redox peaks appeared with mean peak

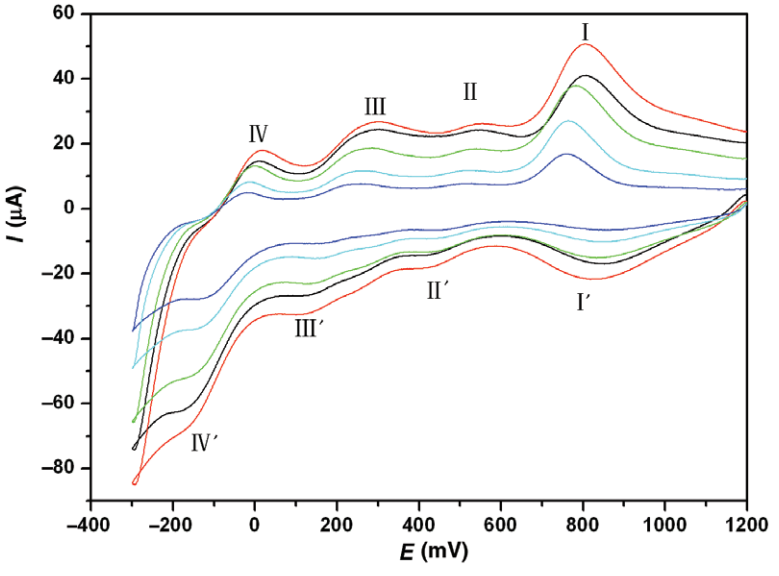

Figure 7. The cyclic voltammograms for **2**-CPE in $H_2SO_4 + Na_2SO_4$ aqueous solution at different scan rate (from inner to outer: 50, 150, 200, 250 mV s^{-1}).

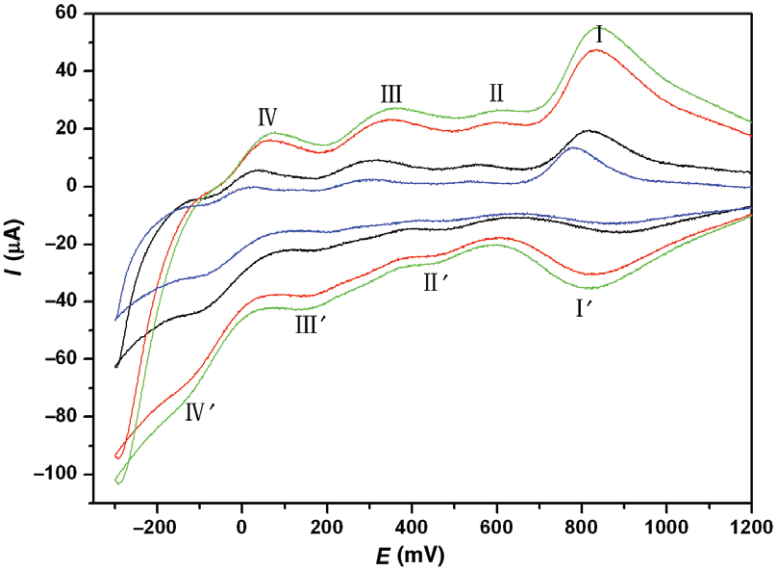

Figure 8. The cyclic voltammograms for **3**-CPE in $H_2SO_4 + Na_2SO_4$ aqueous solution at different scan rate (from inner to outer: 50, 100, 200 mV s^{-1}).

potentials of 837.5, 398.5, 224 and −35 mV. Redox peaks I–I′ should be ascribed to the one-electron redox process of Fe (III/II). Redox peaks II–II′, III–III′, IV–IV′ corresponded to three consecutive two-electron processes of Mo. With the variation

of scan rate from 50 to 200 mV s^{-1}, the change trend in peak currents and peak potentials were similar to **1**-CPE.

4. Conclusions

In summary, we have prepared and structurally characterized three new organic-inorganic hybrid compounds based on the Keggin POMs and iron complex fragments. Complexes **1** and **3** consist of discrete polyoxoanion and counter chiral cation $[Fe(phen)_3]^{3+}$. In **2**, both $[Fe(phen)_2(H_2O)]^{2+}$ groups are coordinated to the α-Keggin-type polyoxoanion $[PMo_{11}^{VI}Mo^{V}O_{40}]^{6-}$ *via* the surface terminal oxygen atoms of two opposite oxygen atoms at the same equator surface. We observed that the stoichiometry plays a key role in the structural control of self-assembly process under the hydrothermal condition and further confirms that molecular design is not clear.

Supplementary materials

Crystallographic data for the structural analysis have been deposited with the Cambridge Crystallographic Data Center, CCDC reference number: 628082, 619071 and 619083. These data can be obtained free of charge at www.ccdc.cam.ac.uk/conts/retrieving.html (or from the Cambridge Crystallographic Data Centre, 12, Union Road, Cambridge CB2 1EZ, UK; Fax: C44 1223/336 033; Email: deposit@ccdc.cam.ac.uk).

Acknowledgements

The authors acknowledge financial support from the National Science Foundation of China (20671016).

References

[1] (a) Y. Wang, J.H. Yu, Y. Du, Z. Shi, Y.C. Zou, R.R. Xu. *J. Chem. Soc. Dalton Trans.*, 4060 (2002); (b) C. Janiak. *Dalton Trans.*, 2781 (2003); (c) B. Moulton, M.J. Zaworotko. *Chem. Rev.*, **101**, 1629 (2001).
[2] (a) V. Soghomonian, Q. Chen, R.C. Haushalter, J. Zubieta. *Science*, **259**, 1596 (1993); (b) N.L. Rosi, J. Eckert, M. Eddaoudi, D.T. Vodak, J. Kim, M. O'Keeffe, O.M. Yaghi. *Science*, **300**, 1127 (2003); (c) Z. Shi, S.H. Feng, S. Gao, L.R. Zhang, G.Y. Yang, J. Hua. *Angew. Chem. Int. Ed.*, **39**, 2325 (2000); (d) R. Kitaura, R.S. Kitagawa, Y. Kubota, T.C. Kobayashi, K. Kindo, Y. Mita, A. Matsuo, M. Kobayashi, H.C. Chang, T.C. Ozawa, M. Suzuki, M. Sakata, M. Takata. *Science*, **298**, 2358 (2002); (e) Y. Wang, J.H. Yu, Y. Du, Z. Shi, Y.C. Zou, R.R. Xu. *J. Chem. Soc. Dalton Trans.*, 4060 (2002).
[3] (a) A. Müller, F. Peters, M.T. Pope, D. Gatteschi. *Chem. Rev.*, **98**, 239 (1998); (b) M. Yuan, Y.G. Li, E.B. Wang, C.G. Tian, L. Wang, C.W. Hu, N.H. Hu, H.Q. Jia. *Inorg. Chem.*, **42**, 3670 (2003); (c) D. Hagrman, C. Zubieta, D.J. Rose, J. Zubieta, R.C. Haushalter. *Angew. Chem. Int. Ed.*, **36**, 873 (1997).
[4] E. Burkholder, V. Golub, C.J. O'Connor, J. Zubieta. *Inorg. Chem. Commun.*, 7363 (2004).
[5] Y. Xu, J.Q. Xu, K.L. Zhang, Y. Zhang, X.Z. You. *Chem. Commun.*, 6153 (2000).

[6] G.Y. Luan, Y.G. Li, S.T. Wang, E.B. Wang, Z.B. Han, C.W. Hu, N.H. Hu, H.Q. Jia. *J. Chem. Soc., Dalton Trans.*, **2**, 233 (2003).
[7] J.Y. Niu, X.L. Wang, J.P. Wang. *Inorg. Chem. Commun.*, **6**, 1272 (2003).
[8] (a) C.M. Liu, D.Q. Zhang, C.Y. Xu, D.B. Zhu. *Solid State Sci.*, **6**, 689 (2004); (b) X.J. Gu, J. Peng, Z.Y. Shi, Y.H. Chen, Z.G. Han, E.B. Wang, J.F. Ma, N.H. Hu. *Inorg. Chim. Acta.*, **358**, 3701 (2005); (c) Z.Y. Shi, X.J. Gu, J. Peng, X. Yu, E.B. Wang. *Eur. J. Inorg. Chem.*, **85**, 385 (2006).
[9] (a) S. Chang, C. Qin, E.B. Wang, Y.G. Li, X.L. Wang, *Inorg. Chem. Commun.*, **9**, 727 (2006); (b) Y.B. Liu, L.M. Duan, X.M. Yang, J.Q. Xua, Q.B. Zhang, Y.K. Lu, J. Liu. *J. Solid State Chem.*, **179**, 122 (2006).
[10] C.R. Deltcheff, M. Fournier, R. Franck, R. Thouvenot. *Inorg. Chem.*, **22**, 207 (1983).
[11] (a) G.M. Sheldrick. SHELX-97, *Program for Crystal Structure Refinement*, University of Göttingen, Germany (1997); (b) G.M. Sheldrick, SHELXL-97, *Program for Crystal Structure Solution*, University of Göttingen, Germany (1997).
[12] (a) Y.P. Ren, X.J. Kong, X.Y. Hu, L.S. Long, R.B. Huang, L.S. Zheng. *Inorg. Chem.*, **45**, 4016 (2006); (b) P.Q. Zheng, Y.P. Ren, L.S. Long, R.B. Huang, L.S. Zheng. *Inorg. Chem.*, **44**, 1190 (2005); (c) Z.Y. Shi, J. Peng, C.J. Gómez-García, B. Benmansour, X.J. Gu, *J. Solid State Chem.*, **179**, 253 (2006); (d) B.X. Dong, J. Peng, Y.H. Chen, Y.M. Kong, A.X. Tian, H.S. Liu, J.Q. Sha. *J. Mol. Struct.*, **788**, 200 (2006).
[13] I.D. Brown, D. Altermatt. *Acta Crystallogy., Sect. B*, **41**, 244 (1985).
[14] A.S.J. Wery, J.M. Gutierrez-Zorrilla, A. Luque, P. Vitoria, P. Roman, M. Martinez-Ripoll. *Polyhedron*, **17**, 1247 (1998).
[15] R. Thouvenot, M. Fournier, R. Franck, G. Rocchiccioli-Deltche. *Inorg. Chem.*, **23**, 598 (1984).
[16] (a) M. Sadakane, E. Steckhan. *Chem. Rev.*, **98**, 219 (1998); (b) Z.G. Han, Y.L. Zhao, J. Peng, Y.H. Feng, J.N. Yin, Q. Liu. *Electroanalysis*, **17**, 1097 (2005); (c) Z.G. Han, Y.L. Zhao, J. Peng, Q. Liu, E.B. Wang. *Electrochim. Acta*, **51**, 218 (2005).